800-MHz High-Performance SAW Filter Using New Resonant Configuration

MITSUTAKA HIKITA, HIROOMI KOJIMA, TOYOJI TABUCHI, AND YASUAKI KINOSHITA, MEMBER, IEEE

Abstract—**A new high-performance surface-acoustic-wave (SAW) filter for use in mobile telephones is presented in this paper. The design for the actual realization of the new filter is examined, from the new filter configuration to the final device operation. A low-loss weighting technique in an interdigital transducer (IDT), a new resonant structure, computer simulation procedures, and material properties are treated. Experimental results with this SAW filter included an 830-MHz center frequency, 3-percent bandwidth, insertion loss of as low as 3.5 ~ 4.0 dB, and 50-dB sidelobe suppression filter.**

I. Introduction

SAW FILTERS OFFER advantages in that they are small, do not need adjustment, and are highly reproducible and reliable [1], [2]. Such devices consist of an input IDT to launch a SAW on a piezoelectric substrate, and an output IDT to reconvert from acoustic to electromagnetic energy. IDT's are also easily made using the standard photolithographic techniques as used for silicon IC's.

A typical application of SAW filters is as TV-IF filters. However, other SAW filter applications, except in such specialized fields as military and satellite communications, have been limited due to their large insertion losses. A unidirectional transducer with three phase drive [3], and a group-type transducer [4] have thus been of particular interest in the search to reduce insertion losses. However, in these transducers, several inductors and capacitors are required to form a matching network. Moreover, a special fabrication process, such as a cross-over for reducing thin metal electrode resistance loss, has been used. Other low-loss nontransversal filters of interest are ring filters [5] and TTR filters [6], [7]. They have very good off-band rejection, but have difficulty in achieving the required frequency response.

Recently, high-performance SAW filters with 1) low insertion loss, 2) sharp cutoff frequency response, and 3) high sidelobe suppression are becoming essential for RF circuit integration in communication equipment such as mobile telephone transceivers, cable TV repeaters, and converters. This paper describes a new high-performance SAW filter that we have developed to meet these needs using several new technologies. The filter is used in a mobile telephone to suppress spurious signals generated in the transmitter mixer.

It has previously been reported that a new weighting approach resulting in a negligible loss increase is possible [8]. We also employed this weighting technique, new phase weighting, in our new filters. A brief explanation will be given in Section III-A.

To realize a sharp cutoff frequency response, a new filter configuration that uses the impedance characteristics of an IDT was developed. To overcome a 6-dB inherent bidirectionality loss, an energy trap resonant structure containing lateral repetitions of the above new configuration as a basic unit, as well as SAW reflectors, is introduced. This new configuration and structure will be discussed in Section III-C.

We chose as a substrate 36°-rotated Y-cut, X-propagated (36° YX-) $LiTaO_3$ (surface shear wave) [9], due to its rather large electromechanical coupling and good temperature coefficients ($k^2 = 2\Delta v/v = 5$ percent, $28 \sim 32$ ppm/°C). Details about substrates will be given in Section IV.

We developed a simplified lattice electric equivalent circuit representation for our new filters to simulate frequency responses. These computer simulation procedures will be given in Section V.

The case presented in this paper is a high-performance SAW filter with a center frequency of 830 MHz, bandwidth of 3 percent, insertion loss of as low as 3.5 ~ 4.0 dB, and sidelobe supression of over 50 dB. These results will be discussed in Section VI.

II. Conventional SAW Filter

The key to realizing an arbitrary frequency response with a conventional SAW filter is to determine the appropriate placements and lengths of the interdigital electrodes [10]. Because an IDT can be regarded as a discrete time-sampling device, a large body of digital-filter theory can be applied to the transducer design. This technique is called apodization and is popularly used. However, there are some problems with it regarding wide application to low-loss SAW filters. They are: 1) an increase in losses, and 2) trade-off between a sharp cutoff frequency response and high sidelobe suppression.

The causes of 1) include a) weighting loss [11], and b) bidirectionality loss. The cause of 2) is as follows. The

Manuscript received October 9, 1984; revised January 30, 1985.

The authors are with the Central Research Laboratory, Hitachi, Ltd., Kokubunji, Tokyo, 185 Japan.

0018-9480/85/0600-0510$01.00 ©1985 IEEE

weighting function, $\sin(x)/x$, provides a sharp cutoff frequency response. However, it is a vibrational function which decreases very slowly. Thus, realization of high sidelobe suppression is difficult because of the finite limitation effect of a window function.

III. Theoretical Treatment of the New Configuration

Realization of a low-loss and sharp cutoff frequency response SAW filter has required two technical breakthroughs. One includes low-loss weighting to synthesize the frequency response and the other concerns a low-loss filter configuration to overcome bidirectionality loss. We have developed a new low-loss weighting technique and new resonant filter configuration. The developed configuration ensures not only very small bidirectionality loss but also a sharp cutoff frequency response.

A. New Phase Weighting Approach

Amplitude weighting (apodization) in an IDT is a technique widely used to provide the desired frequency response. However, this procedure essentially allows weighting loss, because the excited SAW from an amplitude-weighted IDT has nonuniform wave front distortion, as can be seen in Fig. 1(a) [11], [12].

Several new weighting approaches have been proposed to avoid this weighting loss. Withdrawal weighting and distance weighting are two kinds of low-loss weighting approaches which provide uniform SAW wave front distribution [13], [14]. However, it is rather difficult to realize arbitrary weighting functions using these simple weighting techniques. Another low-loss weighting approach, capacitive tap weighting [15], which also provides uniform SAW wave front distribution, requires a special fabrication process to make thin-film SiO_2 dielectric capacitors.

The new low-loss weighting technique [8] that we have developed can achieve an arbitrary weighting function. This is shown in Fig. 1(b). Changes in finger overlaps are used in amplitude weighting to realize a weighting function. The new procedure is also based on changes in finger overlaps. As is illustrated schematically in Fig. 1(b), each finger overlap corresponding to a weighting function is formed continuously from the preceding overlap.

We consider more precisely the difference between conventional amplitude weighting and new phase weighting using an example. $f(x)$, shown in Fig. 1(c), is assumed to be a given weighting function, where x_i's are transversal placements of interdigital electrodes in an IDT. Finger overlaps l_i's in Fig. 1(a) are determined by the relations $l_i = a \cdot f(x_i)$, $i = 1, 2, \cdots$, where a is an arbitrary constant.

Finger overlaps l_i''s (l_i'''s) in Fig. 1(b) are also determined by similar relations. However, a vertical placement of each finger overlap is different from that in Fig. 1(a). It is determined by a placement of the preceding overlap.

For example, finger overlap l_1' in Fig. 1(b), which has the same length as l_1 in Fig. 1(a), is formed continuously from the preceding finger overlap l_2'. l_2', which has the same length as l_2 in Fig. 1(a), is formed continuously from the preceding finger overlap l_3'. As for l_3' and l_3'', the total length $l_3' + l_3''$ has the same length as l_3 in Fig. 1(a), and l_3'' is formed continuously from the preceding finger overlap l_4'. Similar relations hold between l_i' (l_i'') in Fig. 1(b), and l_i in Fig. 1(a). Thus, the weighting in Fig. 1(b) assures almost the same frequency response as for the amplitude weighting in Fig. 1(a).

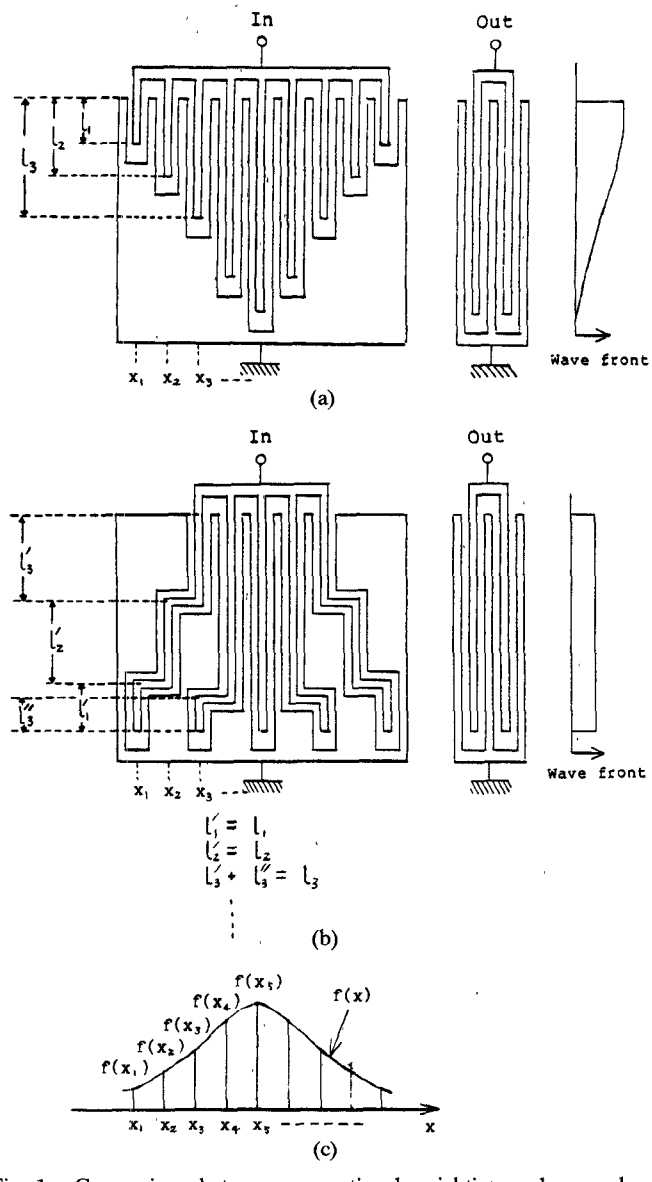

Fig. 1. Comparison between conventional weighting and new phase weighting. (a) Apodization. (b) New phase weighting. (c) Weighting function.

In Fig. 1(b), the propagating SAW receives the same number of excitations along any transversal path in the IDT. Thus, the wave front distribution of the launching SAW from the weighted IDT is approximately planar, as is shown in the figure. The computer simulation proves that at the passband, both the amplitudes and phases of the SAW along each path are nearly equal in quantity.

At the stopband, the difference in amplitudes along each path is not so large, but the in-phases become significant. So, we named this weighting approach "new phase weight-

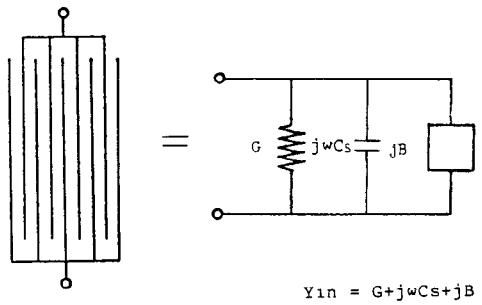

Fig. 2. Electric equivalent circuit for IDT.

ing" because, as stated above, the frequency response of an IDT is primarily determined by the phase differences in the SAW. Since this weighting is based on conventional amplitude weighting, it has a performance almost equivalent to that of the conventional technique. This weighting approach is also suitable for frequency response syntheses of a low-loss SAW filter, due to its planar wave front distribution at the passband.

B. *Image-Impedance Connection of IDT's*

To realize a sharp cutoff frequency response, a new configuration was developed that used the impedance characteristics of an IDT. In order to provide a look at the development background of this configuration, a well-known electric equivalent circuit [16] for an IDT is illustrated in Fig. 2. G represents radiation conductance, Cs represents electric capacitance between fingers in an IDT, and B represents acoustic susceptance due to vibration [16].

From fundamental experiments and computer simulation results, we found that the input impedance of an IDT with $\lambda_0/4$ solid fingers could be classified into three types, according to the number of finger pairs in an IDT. Frequency characteristics for these impedances are shown in Fig. 3. In this figure, N is the number of finger pairs in an IDT, and k^2 is the electromechanical coupling coefficient, which is defined as follows [16]:

$$k^2 = 2(v_f - v_s)/v_s = 2\Delta v/v \quad (1)$$

where v_f is the SAW velocity on the free surface of a substrate, and v_s is the SAW velocity on the shorted (metal coated) surface of a substrate.

Fig. 3(b) shows that if N is optimized, that is, $N \simeq 1.5/k^2$, a wide frequency range exists. Over this range, total susceptance ($\omega Cs + B$) becomes very small due to the cancellation of electric and acoustic susceptance components. As can be seen in Fig. 3(a) and (c), when N is smaller than $1.5/k^2$, total susceptance is capacitive. When, on the other hand, N is larger than $1.5/k^2$, greater inductance is produced.

The new configuration is shown in Fig. 4. One pair of electrically connected IDT's with an optimum number of finger pairs ($N \simeq 1.5/k^2$) is introduced. Input and output IDT's with a broader frequency response are arranged on

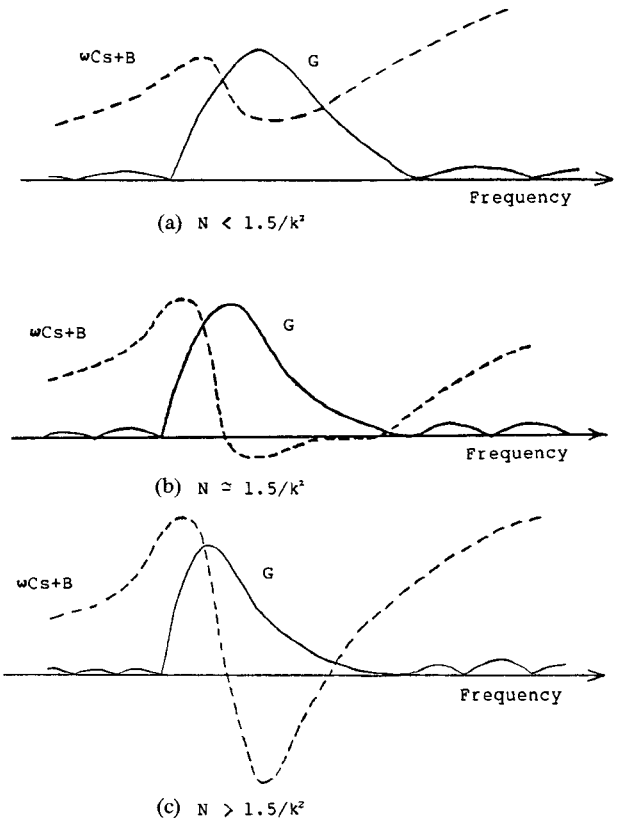

Fig. 3. Frequency characteristics of Yin.

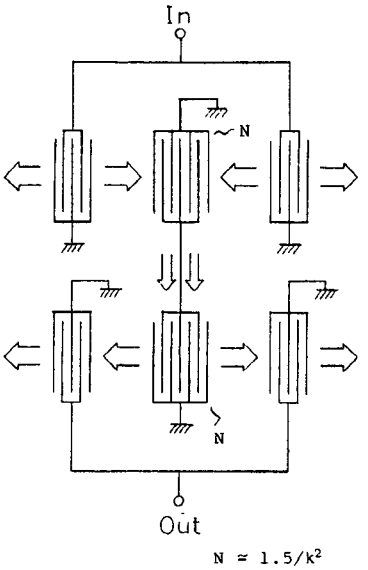

Fig. 4. Realization of sharp cutoff frequency rsponse.

both sides. The electrical connection shown in the figure is called an "image-impedance connection" in circuit theory. With Fig. 4's simple no-weighting configuration, a sharp cutoff frequency response, where the susceptance cancelled frequency range is the passband, can be realized.

This is because if the frequency is within the range where the susceptance is cancelled, the current from an upper image-impedance connected IDT flows into a lower one without reflection, and this range forms the passband of

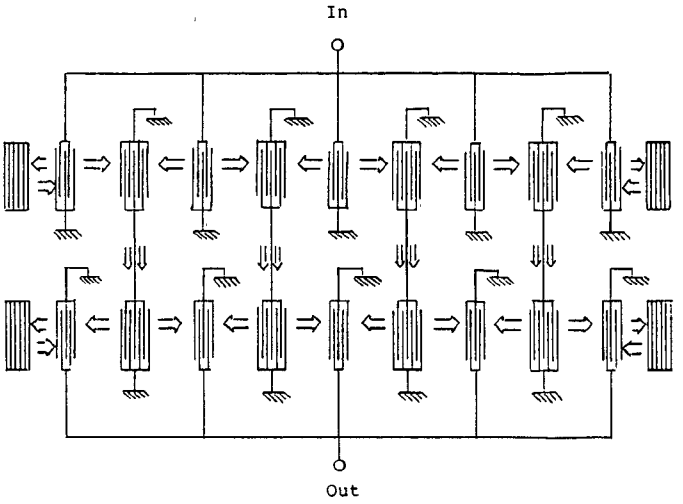

Fig. 5. New filter configuration with low-loss and sharp cutoff frequency response.

the filter. If the frequency is outside this range, almost all current is reflected at the image-impedance connection point because the susceptance component is larger than the conductance component. Consequently, these outside frequency ranges correspond to the stopband of the filter. The transient frequency band is very narrow, so this configuration offers a sharp cutoff frequency response without weighting.

If the numbers of finger pairs in an image-impedance connected IDT are not optimized ($N >$ or $< 1.5/k^2$), large ripples are observed within the passband of the filter. This is because, even in the passband, the current from an upper image-impedance connected IDT is reflected at the connection point due to the influence of the remaining susceptance components. Accordingly, optimization of the number of finger pairs is very important in this configuration.

C. Reduction of Bidirectionality Loss

Fig. 4's configuration allows a 6-dB inherent bidirectionality loss, that is, a 3-dB loss each to the input and output IDT's. To overcome this loss, an energy-trap resonant structure was developed which contained lateral repetitions of Fig. 4 as a basic unit. SAW reflectors were also placed at both ends of the filter.

A schematic illustration of one example of the repetition structure is shown in Fig. 5. Four pairs of image-impedance connected IDT's with an optimum number of finger pairs have been introduced. Input and output IDT's are also divided into five parts. They are arranged between all pairs of image-impedance connected IDT's, and at both ends of the filter there are SAW reflectors, as Fig. 5 shows. In this new configuration, SAW's launching in both directions from the input IDT's are received and regenerated by the image-impedance connected IDT's and return to output IDT's from both sides. This process is schematically illustrated by the arrows in Fig. 5. Thus, a sharp cutoff and low-loss frequency response is obtained by the image-impedance connected IDT's and the lateral repetition structure.

TABLE I
ELECTROMECHANICAL COUPLING COEFFICIENTS (k^2)

Substrate	k^2
Y cut, Z pro. - $LiNbO_3$ (Rayleigh Wave)	4.8 % [23]
128° Y cut, X pro. - $LiNbO_3$ (Rayleigh Wave)	5.5 % [24]
X cut, 112° Y pro. - $LiTaO_3$ (Rayleigh Wave)	0.6 % [25]
64° Y cut, X pro. - $LiNbO_3$ (Surface Shear Wave)	11.3 % [20]
41° Y cut, X pro. - $LiNbO_3$ (Surface Shear Wave)	17.2 % [20]
36° Y cut, X pro. - $LiTaO_3$ (Surface Shear Wave)	5.0 % [9]

IV. SUBSTRATE MATERIAL

The electromechanical coupling coefficient k^2 limits the maximum bandwidth of the filter. This is because the optimum number of finger pairs (N) is determined by the relation $N \simeq 1.5/k^2$. k^2's for various substrate materials are summarized in Table I.

Rayleigh waves (RW) have been popularly used in recent SAW filters. However, surface shear waves (SSW) appear to have several advantages even though exact SSW definitions have still not been made. Surface skimming bulk waves (SSBW) and leaky surface waves (LSW) are other names for surface shear waves [17]–[20].

The penetration depth of SSW's propagating on the free surface of a substrate is very large (several wavelengths). If the surface of the substrate is coated with thin metal film (shorted surface), strong energy trapping can be realized. So, for some substrates, such as $LiNbO_3$ and $LiTaO_3$, the electromechanical coupling coefficient (k^2) of SSW's is greater than that for RW's.

The propagation loss of SSW's, which is a little larger than that of RW's [21], reveals no serious problems for their applications to SAW filters. In fact, we have already published a report about another type of low-loss SAW filter (a TTR filter, loss = 2 ~ 4 dB) using SSW's (64° YX–$LiNbO_3$, 36° YX–$LiTaO_3$) [6], [7]. The propagation loss contribution was negligibly small (0.2 ~ 0.5 dB).

We have also shown that the mixed field equivalent circuit model is accurate enough to electrically represent an IDT for SSW's [7]. The mixed field model is an intermediate model between Smith's crossed field model and the in-line field model [16]. In it, the negative capacitance coefficient (α) plays a very important part.

From Table I, we determined that to realize the bandwidth for a mobile telephone (BW = 20 MHz, $f_0 = 830$ MHz), 128° YX-$LiNbO_3$ and 36° YX-$LiTaO_3$ were the best choices. In the experiment, 36° YX-$LiTaO_3$ (SSW) was chosen as a substrate, because of its rather good temperature coefficient (28 ~ 30 ppm/°C, cf. 80 ppm/°C for 128° YX-$LiNbO_3$).

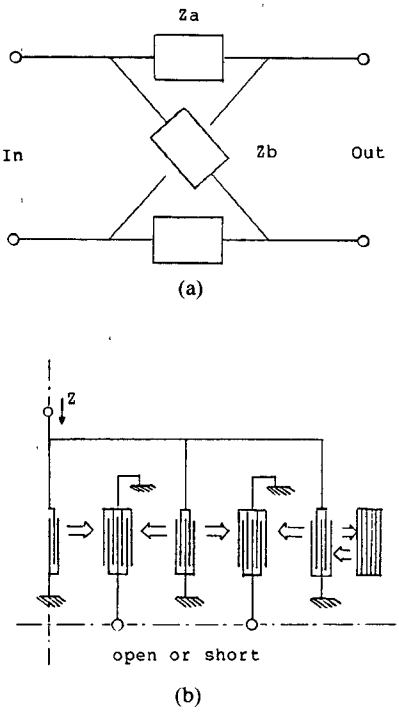

Fig. 6. Equivalent circuit representation for Fig. 5's configuration. (a) Lattice equivalent circuit. (b) Quarter part of the filter.

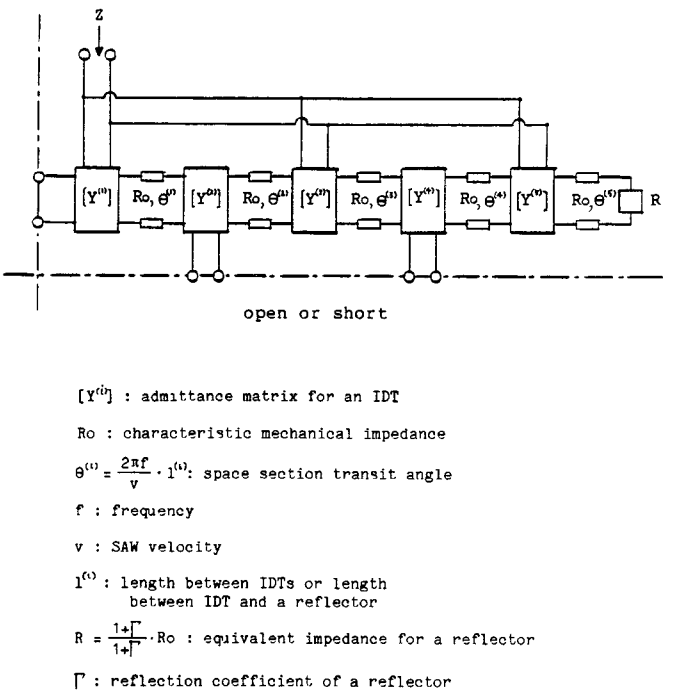

Fig. 7. Electric equivalent circuit for Fig. 5(b)'s quarter part of the filter.

V. Computer Simulation Procedure

The configuration shown in Fig. 5 is rather complicated, so it would be difficult to design the filter without taking advantage of computer simulation. A lattice equivalent circuit representation for Fig. 5's structure is possible due to the symmetric properties of the filter, shown in Fig. 6(a). In the figure, *Za* and *Zb* are short and open half section impedances, respectively, which can be estimated from the quarter part of the filter (see Fig. 6(b))

$$Za = \frac{1}{2}Z(\text{short}) \tag{2a}$$

$$Zb = \frac{1}{2}Z(\text{open}). \tag{2b}$$

Z(short) and Z(open) are the electric impedances of Fig. 6(b)'s configuration, where the image-impedance connection points are, respectively, short and open.

The electric equivalent circuit for Fig. 6(b)'s quarter part of the filter is shown in Fig. 7. The admittance matrix for IDT, $[Y^{(i)}]$, can be formulated by using a mixed field equivalent circuit model [7]. Thus, it is not a very complicated problem to mathematically formulate *Za* and *Zb* using Fig. 7's equivalent circuit. Computer calculations of frequency responses are also possible using *Za*, *Zb*, and Fig. 6(a)'s lattice circuit.

Simulation results employing Fig. 5's four-repetition structure and with 36° YX-$LiTaO_3$ as a substrate are shown in Fig. 8. The negative capacitance coefficient (α) used in the mixed field circuit model is 0.5. The parameters

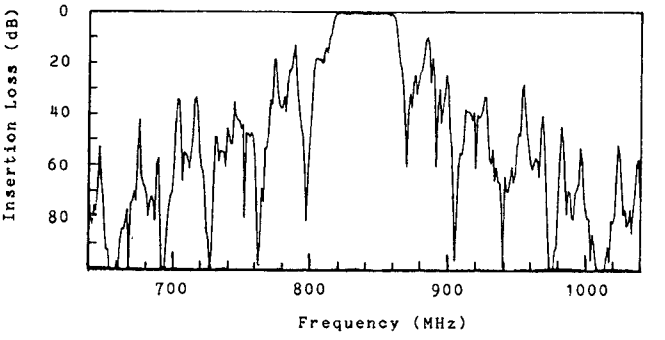

Fig. 8. Computer simulation results for new filter configuration (without weighting).

assumed in the simulation are as follows:

N_I (image-impedance connected IDT) = 26 (3a)

N_{IO} (input and output IDT) = 10 (3b)

N_R (reflector) = 10 (short metal finger pairs) (3c)

W (aperture of the filter) = 30 wavelengths (3d)

S_{II} (space between IDT's) = 4 wavelengths (3e)

S_{IR} (space between IDT and reflector) = 3/8 wavelength. (3f)

A sharp cutoff frequency response with a bandwidth of 5 percent and low insertion loss was achieved without weighting. A wider frequency bandwidth would be possible if a substrate with a larger electromechanical coupling coefficient was employed. For example, a bandwidth of more than 10 percent could be obtained using 41° YX-$LiNbO_3$ [22].

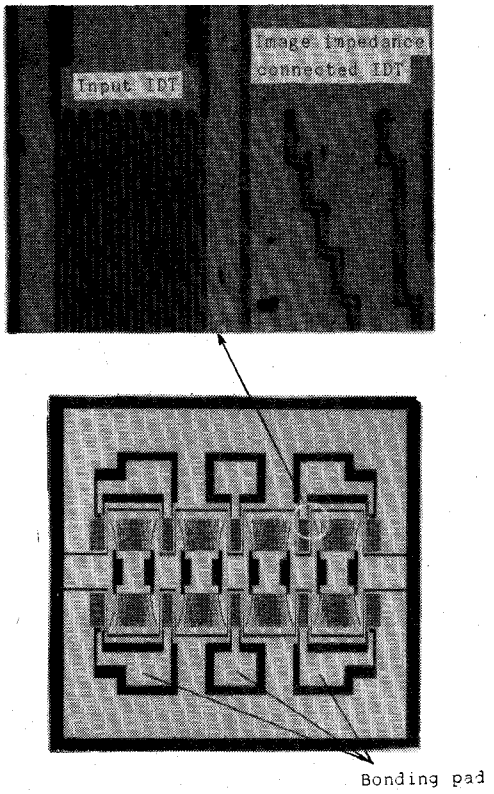

Fig. 9. Mask pattern employed in the experiment.

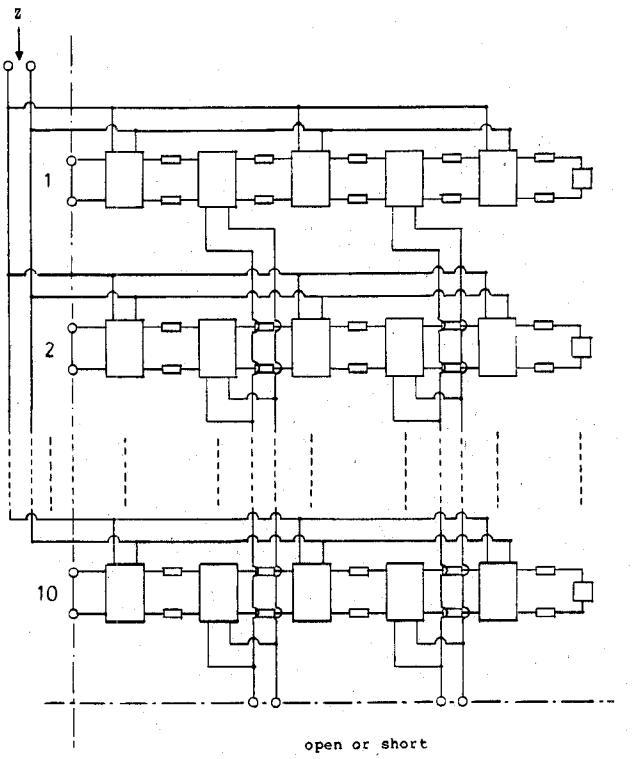

Fig. 10. Electric equivalent circuit for the quarter part of Fig. 9's filter configuration.

A reflector with 10 short metal finger pairs is not sufficient to reduce leakage loss to the limit. There are two ways to achieve lower leakage loss. One is to increase the number of short metal finger pairs in the reflector, and the other is to introduce more repetitions. However, the former causes a narrowing of the bandwidth of the filter and the latter increases the chip size. As a result of these considerations and the computer simulations, a four-repetition structure with reflectors having 10 short metal finger pairs was chosen for use in a mobile telephone.

VI. Application to Mobile Telephone Transceiver

The new filter that has been developed was used in the transmitter circuit of a mobile telephone to reduce spurious signals generated in the mixer. Since a cascade-connected semi-coaxial resonator filter was used in this circuit, almost the same performance as a conventional filter is required. Requirements included 1) low insertion loss (below 6 dB), 2) sharp cutoff frequency response, and 3) high sidelobe suppression (over 50 dB). By applying new phase weighting to image-impedance connected IDT's and using sophisticated computer simulation techniques, a high-performance SAW filter was achieved that could replace the conventional semi-coaxial filter.

A. Mask Pattern Design

A photograph of the mask pattern developed for the mobile telephone transceiver is shown in Fig. 9. A four-repetition structure (four pairs of image-impedance connected IDT's) was employed. Input and output IDT's are also divided into five parts and arranged between all pairs of image-impedance connected IDT's. They are drawn out to three bonding pads, as can be seen in the photograph.

Fig. 5's configuration in itself offers low insertion loss and sharp cutoff frequency response. However, to achieve high sidelobe suppression, weighting must be introduced to the IDT's. We thus introduced the new phase weighting for image-impedance connected IDT's, as shown in the photograph.

The pattern has been designed using 36° YX-$LiTaO_3$ as a substrate. A Hamming function with ten vertical divisions was employed as the weighting function because it provides high sidelobe suppression near the main lobe

$$H(x) = 0.54 + 0.46\cos(\pi x), \qquad |x| \leqslant 1.0. \tag{4}$$

The transversal length for an image-impedance connected IDT is 46 wavelengths due to the weighting. However, the effective number of finger pairs is 26, which is the same number as in Fig. 8's simulation. The other parameters are also the same as used in Fig. 8's simulation.

The similar lattice equivalent circuit representation for the filter like the one in Fig. 6(a) is also possible. An electric equivalent circuit for the quarter part of Fig. 9's filter configuration is shown in Fig. 10. As stated above, ten vertical divisions were employed to realize the weighting function (Hamming function). Thus, in Fig. 10, we introduced ten electric equivalent circuits, each of which corresponds to the SAW path. These equivalent circuits are electrically connected in parallel. It is also possible to formulate *Za* and *Zb* for lattice equivalent circuits using the same procedures as used in Fig. 8's simulation.

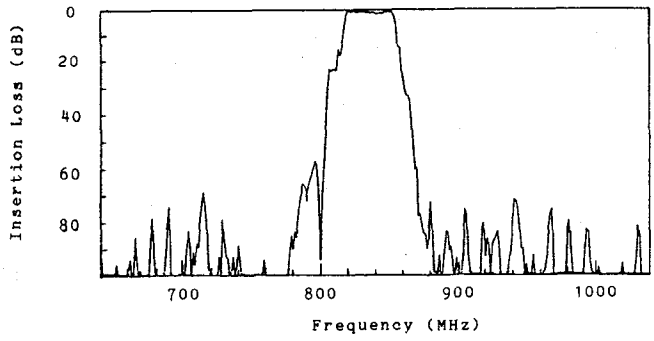

Fig. 11. Computer simulation results of filter for mobile telephone.

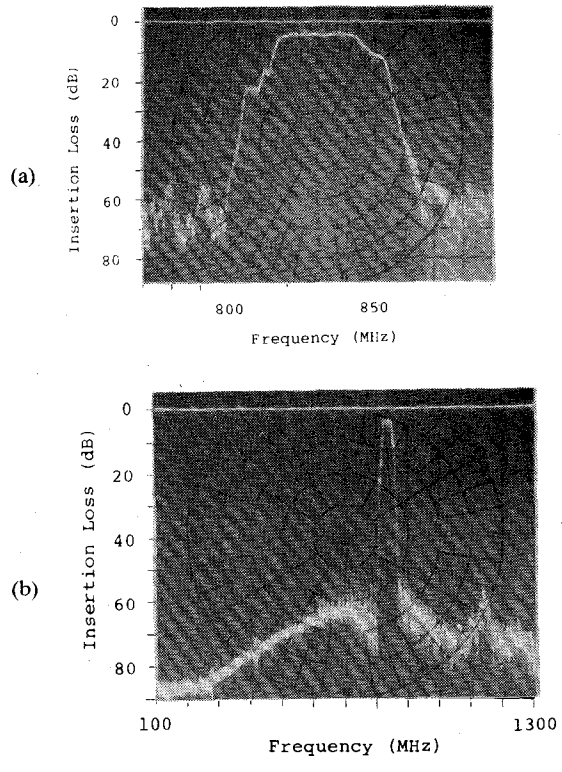

Fig. 12. Experimental results of filter for mobile telephone. (a) Passband characteristics. (b) Out-of-band characteristics.

Computer simulation results that were used to design the filter for the mobile telephone transceiver are shown in Fig. 11. High sidelobe suppression is achieved and the required frequency responses are satisfied. As will be shown in Section VI-B, fairly good agreement between simulation and experimental results is obtained. Highly accurate computer-aided design of low-loss SAW filters was attained.

B. Experimental Filter

Experimental results with an 830-MHz center frequency and 25 ~ 27-MHz bandwidth (1-dB down) are shown in Fig. 12. A high-performance filter was achieved that had a loss of as low as 3.5 ~ 4.0 dB, sharp cutoff frequency response, and high sidelobe suppression (over 50 dB). Passband ripples were smaller than 0.3 dB. All the frequency response requirements for the mobile telephone transceiver can be satisfied over a wide temperature range.

TABLE II
CHARACTERISTICS OF FILTER FOR MOBILE TELEPHONE

Center Frequency	830 MHz
Bandwidth (-1 dB)	25~27 MHz
Insertion Loss	3.5~4.0 dB
Pass Band Ripple	± 0.3 dB
Sidelobe Suppression	> 50 dB
Pattern Size	1.5×1.6 mm
Minimum Finger Width	1.2 μm
Al Thickness	0.1 μm
Substrate	36°YX - $LiTaO_3$ (k^2=5 %)
Temperature Coefficient	28~ 32 ppm/°C
Temperature Range	-36°~+80° C

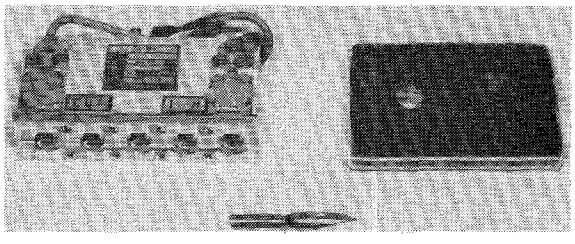

Fig. 13. Comparison between conventional semi-coaxial filter and new SAW filter.

All characteristics clarified in the experiment are summarized in Table II. Aluminum electrodes with a 1.2-μm minimum finger width and 0.1 μm thickness were used, making it possible to utilize the same standard photolithographic techniques as are used for silicon IC's (e.g., optical contact or projection exposure and chemical etching processes). This filter offers not only high-performance but also very high mass-producibility and reliability.

C. Comparison with Conventional Technology

A comparison between a conventional semi-coaxial filter for the mobile telephone transceiver and the new SAW filter is shown in Fig. 13. The photo on the left shows the SAW filter mounted on a TO-5 package, while the one on the right is hermetically sealed.

Because the size of the SAW filter is about one one-hundredth that of a conventional coaxial filter, it offers several advantages. Not only does it meet the frequency response requirements for the mobile telephone transceiver, but it also provides wider applicability to RF circuit integration in communication equipment.

VII. CONCLUSION

1) New phase weighting provides launching SAW with planer wave front distribution at the passband of the filter. It offers not only performance nearly equivalent to that of amplitude weighting, but also low-loss frequency response synthesization.

2) Utilization of laterally repeated structure implementing one pair of image-impedance connected IDT's as a basic unit offers low loss as well as sharp cutoff response.

3) A high-performance SAW filter which was achieved by applying a new phase weighting technique to image-impedance connected IDT's not only assures low loss (3.5 ~ 4.0 dB) and high sidelobe suppression (over 50 dB) but also satisfies all the frequency response requirements for a mobile telephone transceiver.

4) 36° YX-$LiTaO_3$ was employed as a substrate in the experiment. The standard optical contact exposure and chemical-etching processes were used to form aluminum 1.2 μm electrodes.

ACKNOWLEDGMENT

The authors gratefully acknowledge the many useful discussions and considerable help of M. Toya of Hitachi Ltd.'s Totsuka Works, Y. Fujiwara of Hitachi Denshi Ltd., T. Toyama of Hitachi Ltd.'s Yokohama Works, and T. Hazama of Hitachi Ltd.'s Consumer Research Center. Thanks are also due to A. Sumioka for testing the filter, H. Onozato for the photolithography process, and K. Chiba for the device fabrications.

REFERENCES

[1] *Proc. IEEE* (Special Issue on Surface Acoustic Wave Devices and Applications), vol. 64, 1976.
[2] A. J. Slobodnik, Jr., T. L. Szabo, and K. R. Laker, "Miniature surface-acoustic-wave filter," *Proc. IEEE*, vol. 67, p. 129, 1979.
[3] B. R. Potter, "*L*-Band low loss SAW filters," in *IEEE Ultrason. Symp. Proc.*, 1979, p. 533.
[4] K. Yamanouchi, F. Nyffer, and K. Shibayama, "Low insertion loss acoustic surface wave filter using group-type unidirectional interdigital transducers," in *IEEE Ultrason. Symp. Proc.*, 1975, p. 317.
[5] F. Sandy and T. E. Parker, "Surface-acoustic-wave ring filter," in *IEEE Ultrason. Symp. Proc.*, 1976, p. 391.
[6] Y. Kinoshita, M. Hikita, T. Tabuchi, and H. Kojima, "Broadband resonant filter using surface-shear-wave mode and twin-turn reflector," *Electron. Lett.*, vol. 15, p. 130, 1979.
[7] M. Hikita, Y. Kinoshita, H. Kojima, and T. Tabuchi, "Resonant S.A.W. filter using surface shear wave mode on $LiTaO_3$ substrate," *Electron. Lett.*, vol. 16, p. 446, 1980.
[8] M. Hikita, Y. Kinoshita, H. Kojima, and T. Tabuchi, "Phase weighting for low loss SAW filters," in *IEEE Ultrason. Symp. Proc.*, 1980, p. 308.
[9] K. Nakamura, M. Kazumi, and M. Shimizu, "SH-type and Rayleigh-type surface wave on rotated Y-cut $LiTaO_3$," in *IEEE Ultrason. Symp. Proc.*, 1979, p. 404.
[10] R. H. Tancrell and M. G. Holland, "Acoustic surface wave filters," *Proc. IEEE*, vol. 59, p. 393, 1971.
[11] R. A. Waldron, "Power transfer factors for nonuniformly irradiated interdigital piezoelectric transducers," *IEEE Trans. Sonics Ultrason.*, vol. SU-19, p. 448, 1972.
[12] W. Mader, H. Stocker, and G. Tobolka, "Diffraction in TV-IF filter using multistrip coupler," in *IEEE Ultrason. Symp. Proc.*, 1980, p. 294.
[13] K. Kogan and P. Romik, "SAW bandpass filter with withdrawal weighting transducers," in *IEEE Ultrason. Symp. Proc.*, 1980, p. 302.
[14] K. Yamanouchi, E. Neguro, and K. Shibayama, "Acoustic surface wave filters using new distance weighting techniques," in *IEEE Ultrason. Symp. Proc.*, 1980, p. 313.
[15] D. C. Malocha and B. J. Hunsinger, "Capacitive tap weighted SAW transducers," *IEEE Trans. Sonics Ultrason.*, vol. SU-24, p. 293, 1977.
[16] W. R. Smith, F. M. Gerard, J. C. Collins, T. M. Reeder, and H. J. Shaw, "Design of surface wave delay lines with interdigital transducers," *IEEE Trans. Microwave Theory Tech.*, vol. MTT-17, p. 865, 1969.
[17] T. I. Browning, M. F. Lewis, and R. F. Milson, "Surface acoustic waves on rotated Y-cut $LiTaO_3$," in *IEEE Ultrason. Symp. Proc.*, 1978, p. 586.
[18] K. H. Yen, K. F. Lau, and R. S. Kagiwada, "Shallow bulk acoustic wave filter," in *IEEE Ultrason. Symp. Proc.*, 1978, p. 680.
[19] K. H. Yen, K. F. Lau, and R. S. Kagiwada, "Recent advances in shallow bulk acoustic wave devices," in *IEEE Ultrason. Symp. Proc.*, 1979, p. 776.
[20] K. Yamanouchi and K. Shibayama, "Propagation and amplification of Rayleigh waves and piezoelectric leaky waves in $LiNbO_3$," *J. Appl. Phys.*, vol. 43, p. 856, 1972.
[21] H. Kojima, Y. Kinoshita, M. Hikita, and T. Tabuchi, "Velocity, electromechanical coupling factor and acoustic loss of surface shear waves propagating along *X*-axis on rotated Y-cut plates of $LiNbO_3$," *Electron. Lett.*, vol. 16, p. 445, 1980.
[22] M. Hikita, H. Kojima, T. Tabuchi, and Y. Kinoshita, "New low-loss, broad-band SAW filter using unidirectional IDT's with U-shaped MSC's" to be published in *Electron. Lett.*
[23] B. A. Auld, *Acoustic Fields and Waves in Solids*, vol. 2. New York: Wiley, 1973.
[24] K. Shibayama, K. Yamanouchi, K. Sato, and T. Neguro, "Optimum cut for rotated Y-cut $LiNbO_3$ crystal used as the substrate of acoustic-surface-wave filters," *IEEE Proc.*, vol. 64, p. 595, 1976.
[25] Catalog of Toshiba Corporation for $LiTaO_3$ Single Crystals.

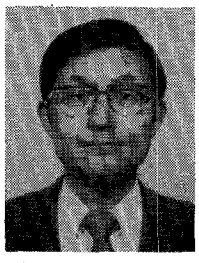

Mitsutaka Hikita received the B.S., M.S., and Ph.D. degrees in electronics engineering, all from Hokkaido University, Sapporo, Japan, in 1972, 1974, and 1977, respectively.

In 1978, he joined Central Research Laboratory, Hitachi, Ltd., Tokyo, Japan. From 1972 to 1978, he was engaged in research works on the analysis of electromagnetic-field problems, microwave accoustics, and acoustooptic interactions. From 1978 to 1983, he worked on high-performance SAW filters for radio communication equipments. Recently, he has been engaged in RF system design for cellular radio, as well as advanced application of SAW technologies.

Dr. Hikita is a member of the Institute of Electronics and Communication Engineers of Japan.

Hiroomi Kojima was born in Aomori, Japan, on August 26, 1936. He received the B.S. and M.S. degrees in physics from the University of Gakushuin, Japan, in 1960 and 1962, respectively.

Since joining the Central Research Laboratory, Hitachi Ltd., Tokyo, in 1962, he has been engaged in research on laser application devices, liquid crystal devices, and surface acoustic wave devices.

Mr. Kojima is a member of the Japan Society of Applied Physics, the Physical Society of Japan, and the Institute of Electronics and Communication Engineers of Japan.

Toyoji Tabuchi graduated from the Electric course of Tadotsu Technical High School, Kagawa, Japan in 1967.

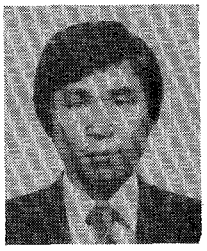

He joined Central Research Laboratory, Hitachi Ltd., Tokyo, in 1967, and has been engaged in research on laser application devices, liquid crystal devices, and surface acoustic wave devices.

Mr. Tabuchi is a member of the Institute of Electronics and Communication Engineers of Japan.

✠

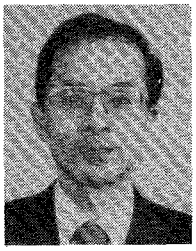

Yasuaki Kinoshita (S'62–M'67) received the B.S., M.S., and Ph.D. degrees in electrical engineering from Hokkaido University, Sapporo, Japan, in 1959, 1964, and 1967 respectively.

From 1967, he was a Lecturer at Hokkaido University and joined Central Research Laboratory, Hitachi Ltd., Tokyo in 1968. Since 1977, he has been a Visiting Professor at Chiba University, Chiba. He is currently a Senior Researcher at the laboratory, where he has engaged in research and development of low-loss SAW filters and their applications. He has done development work in the field of millimeter-wave parametric amplifiers and optical fibers, and studied technological forecasting of telecommunication technologies.

Dr. Kinoshita is a member of the Institute of Electronics and Communication Engineers of Japan.